Modelling Velocity Profiles using the Law of the Wake for Tidal Currents and Winds

Richard H. Karsten[1] and Lilli F. Enders[2]

1. Department of Mathematics and Statistics, Acadia University
2. Department of Earth, Atmospheric and Planetary Sciences, Massachusetts Institute of Technology

Keywords—**vertical profiles, power law, law of the wake, ADCP, tidal flow, wind speed.**

I. Introduction

THE high-energy flow at potential tidal and wind energy sites generates turbulent boundary layers that extend across the height of turbines. Understanding and characterizing the vertical profiles of the flow in the boundary layer is important for optimizing turbine performance and improving flow modelling. In this work we examine two models of the vertical profiles: the standard power law given by equation (1) and the law of the wake, formed by adding a wake function to the standard law of the wall, given by equation (2). Most previous tidal studies, for example [1] and [2], have focused on the applying the power law for this purpose. More recently, Milne et al. [3] used the "law of the wake" first introduced by Coles [4]. In [5], we compare the two approaches by examined the vertical profiles of ADCP data from the Minas Passage, Bay of Fundy. Flow in Minas Passage routinely exceeds 5 m/s and is highly turbulent ($Re \approx 10^8$) [6], an ideal location to examine the theories of turbulent boundary layers. Here we recount some of those results and extend the comparison to a wind data set to determine. Our goal is to better understand the two models, and how they can be applied to ensemble averages.

A. ADCP and Wind Data

The tidal current velocity data considered here are derived from three Acoustic Doppler current profiler (ADCP) deployments at the FORCE CLA in the northern portion of the Minas Passage. A single five-beam Nortek Signature 500 kHz ADCP was deployed three times on a stationary platform. The ADCPs were deployed within 25 m of each other, on a volcanic platform that is relatively flat with a mean water depth between 35 to 40m. A full description of the deployments and analysis of the data can be found in [6]. The data analysed here are 5-minute ensemble averages, taken every 15 minutes. Table 1 lists the details of the three deployments, including the number of ensemble-mean vertical profiles used in the analysis.

For the wind data, we use three years of data (2013, 2019, 2020) from the Cabauw Experimental Site for Atmospheric Research [7]. We choose this dataset since it is well studied and easy to access. The data set records the average wind speed of 10-minute ensembles, at 6 heights up to a maximum of 200 m. One year of data roughly matches the time span of the ADCP data set and gives over 17,000 high-speed profiles, see Table 1. We choose to examine 3 years of data to see if the analysis would vary over different years.

Table 1 Data properties. The profiles column lists the number of ensembles that exceed the minimum speed requirements.

	Start Date	*Days*	*Depth/ Height*	*Profiles*
ADCP A	2017-12-14	65	38 m	4,749
ADCP B	2018-03-30	53	36 m	3,739
ADCP C	2018-09-15	74	38 m	5,352
Wind 2013	2013-01-01	365	200 m	17,879
Wind 2019	2019-01-01	365	200 m	17,976
Wind 2020	2020-01-01	365	200 m	20,731

B. Previous Studies

Determining the form of the mean vertical profile of turbulent flow has a long history, going back to the work of von Kármán and Prandtl. But there is still considerable discussion about whether the laws are "universal" or dependent on Reynolds number, and whether the laws can be rigorously derived or established empirically (for example, see the discussion in [8]).

The "law of the wall" is often used to describe the velocity near the bottom, in what is called the logarithmic boundary layer. The law of the wall has been shown to accurately model the bottom boundary layer in tidal flows [9], [10], but it generally does not extend through the entire water column.

On the other hand, the "power law," given in (1), is used to model the entire water column. Even though it satisfies the no-slip condition at the bottom, it is often thought that the "validity of this power formula ceases in the immediate neighborhood of the wall."[11] Recent application of the power law to tidal flows include Lewis

et al. [1], who examined the vertical profiles of two ADCPs in the Irish Sea, and Sentchev et al. [2], who examined the vertical profiles from a single ADCP in Alderney Race.

There is also a less-known model introduced by Coles [4]: the "law of the wake," given in (2). Coles found that the velocity deficit outside the boundary layer had a consistent form, with dynamics similar to that of a wake. For simplicity we will refer to this as the "wake law." The wake law can be seen as an extension of the law of the wall beyond the logarithmic boundary layer, to the entire water column. More recently, the wake law has been discussed by Schultz and Flack [12] and a number of works by Guo [13]. In terms of tidal flows, Milne et al. [3] used the wake law to examine the vertical profile of ADCP data deployed in Pentland Firth.

In terms of the atmospheric boundary layer, both the law of wall (or log law) and the power law are standard tools for analyzing vertical profiles [14]. Often the log law is adapted to add a stability correction function related to the thermal stability of the boundary layer [15]. In practice, this function plays a similar role to the wake function extending of the law of the wall beyond the logarithmic boundary layer. However, the wake law has not been used extensively in atmospheric studies.

C. *Paper Summary*

In this work, we examine the vertical profiles of the flow from tidal and wind data sets discussed above. We examine both short and long time means of the data. We compare the power law to wake law in terms of the quality of fit and the variation in the model parameters.

II. METHODS

D. *Normalizing data*

Normalization of the vertical profiles is a critical step in the following analysis as it allows for the comparison and averaging of vertical profiles under different conditions and with different mean speeds. The top plot in Fig. 1 shows the signed speed for 3 days of data from ADCP A during a spring tide. The tidal range has a maximum value of 13.5 m over this time frame. Only data below a threshold of 82.5% of the total water depth was used, in order to remove data contaminated by sidelobe interference (see [6] for details).

The use of a normalized vertical coordinate is standard in the analysis of turbulent boundary layers, but the choice of vertical coordinate can vary depending on whether the focus is the inner or outer boundary layer (see for example [12]). Since the tidal range at the site is so large and we are focused on the entire water column, it is useful to use a scaled vertical variable, $\eta = z/h$, where h is the mean water depth for the ensemble, so that $0 \leq \eta \leq 1$. For each ensemble, the ADCP data is interpolated onto a constant grid in η as shown in the middle plot in Fig. 1.

Finally, we normalize the speeds by the depth averaged speed at each time. We only consider the non-slack flow, when ebb speeds exceed 1.25 m/s and flood speeds exceed 1.5 m/s. Approximately 75% of all the ensembles meet this criterion. The result is show in the bottom plot of Fig. 1. Through this normalization process, nearly all indication of the tidal cycle has been removed. It is therefore reasonable to think that the vertical profiles can be represented by a function of η, that varies little over time.

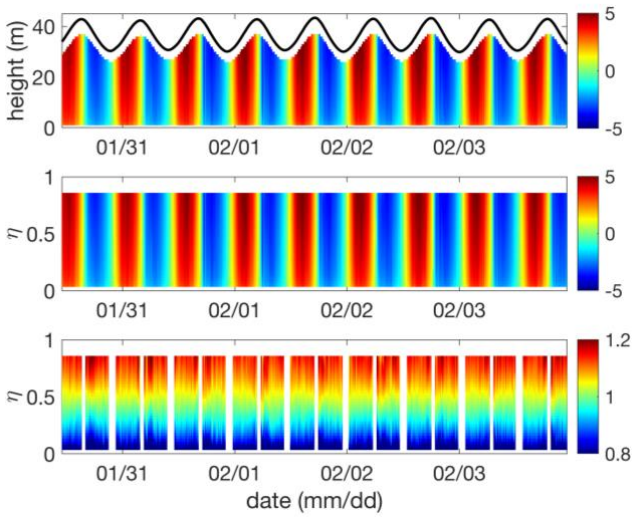

Fig. 1 Data from ADCP A for 3 days in 2018. Top, signed speed (m/s) vs height above the bottom; middle, signed speed (m/s) vs $\eta = z/h$; bottom, speed normalized by the depth average speed vs η.

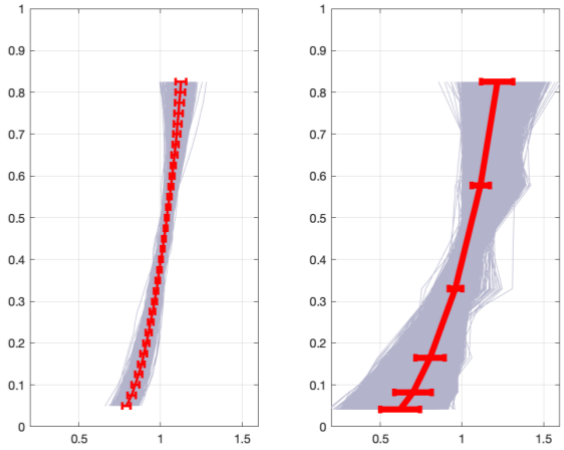

Fig. 2 Normalized vertical profiles of tidal speed (left) and wind speed (right). The individual ensemble average curves are plotted in grey: 3,036 ensembles for ADCP A flood on the left and 20,731 wind ensembles from 2020 o the right. For both plots the mean of the ensemble curves is plotted in red, with error bars of one standard deviation.

For the wind data set used here, the normalization process is chosen to mimic that used for the tidal data. The heights for all measurements are fixed, with a maximum height of 200 m. We choose the value of η for the highest measured level equal to the highest level of measurement for the ADCPs, giving $\eta = \frac{z}{200}(0.825)$. Then, as with the ADCP data, we normalize the speeds by the depth averaged speed at each time. Again, we only consider cases of strong flow, where the depth averaged wind

speed exceeds 8m/s. For the wind data, only 35% of the profiles over the three years exceed this limit.

The normalized profiles for ADCP A flood tide and the 2020 wind data set are shown in Fig. 2. For the ADCP data, the normalization process has collapsed the 3000 profiles onto nearly a single profile; the maximum coefficient of deviation (standard deviation/mean) is only 3%. For the wind data, the profiles do share a common profile but there is considerably more variation with a maximum coefficient of deviation of 19%. The mean profiles for both data sets have similar properties suggesting that a similar profile model may work.

E. Models of the Vertical Profiles

As mentioned above, we will examine two models of the vertical profiles: the power law and the wake law. The power law can be written as

$$u(\eta) = \left(\frac{\eta}{\beta}\right)^{\frac{1}{\alpha}}, \tag{1}$$

where α is the power/exponent. The parameter β is discussed in different ways but can be thought of as a reference height, since $u(\beta) = 1$.

The law of the wake is formed by adding a wake function to the standard law of the wall:

$$u(\eta) = \frac{u_*}{\kappa}[\ln(\eta) + B + \Pi\, w(\eta)], \tag{2}$$

where u_* is the friction velocity, $\kappa = 0.41$ is the von Kármán constant, B is a parameter that shifts the vertical profile but does not affect its shape, $w(\eta)$ is the wake function and Π is the amplitude of the wake function. It is useful to interpret the friction velocity in terms of a bottom drag,

$$C_D = \left(\frac{u_*}{U}\right)^2, \tag{3}$$

where U is a reference velocity, here chosen to be the depth averaged velocity.

The wake function has been chosen in previous studies to have many forms, but most often is chosen to satisfy the following conditions:

$$w(0) = w'(0) = w'(1) = 0, w(1) = 1. \tag{4}$$

That is, the wake function has minimal effect on the flow near the bottom so that the near-bottom flow is determined by the law of the wall. Here we choose the cubic wake function:

$$w(\eta) = \eta^2(3 - 2\eta). \tag{5}$$

There are other possible choices (see [12]), but they have a similar shape and do not significantly change the results.

For the power law, there are two unknown parameters, α and β; for the wake law, there are three, u_*, B, and Π. The parameters for each model are fit to the data using MATLAB's fminsearch function to minimize the sum of the squared error.

III. Results

F. Mean Profiles

We first consider the averages of all ebb and flood ensembles for each ADCP and the average of all ensembles for each year of the wind data. These correspond to the mean profiles shown in red in Fig. 2. The error for the curve fits for these long-time means are given in Table 2 in the rows labelled Mean and parameter values are shown as outlined markers in Fig. 4 and Fig. 5. For these average profiles, the root mean square error (RMSE) is always small, at most 1.6%. The RMSE for the wake law is always smaller than the power law, particularly for the tidal flow.

TABLE 2 THE RMSE (%) FOR THE PROFILE CURVE FITS AS A PERCENTAGE. VARIATIONS ARE ONE STANDARD DEVIATION.

ADCP/ Wind		Wake Law		Power Law	
		Flood	Ebb	Flood	Ebb
A	Mean	0.14	0.17	1.1	1.0
	Ensembles	0.65±0.31	0.8±0.45	1.35±0.62	1.43±0.65
B	Mean	0.12	0.23	0.75	0.74
	Ensembles	1.0±0.69	0.96±0.65	1.45±0.78	1.40±0.82
C	Mean	0.15	0.26	1.1	0.44
	Ensembles	0.81±0.36	0.91±0.48	1.45±0.57	1.30±0.66
13	Mean	0.95		1.6	
	Ensembles	3.4±4.2		5.6±5.8	
19	Mean	1.1		1.6	
	Ensembles	3.5±3.9		5.8±5.8	
20	Mean	0.84		1.6	
	Ensembles	3.5±4.4		5.9±6.4	

G. Ensemble Profiles

We next examine fitting curves to each ensemble average profile. The mean RMSE for these fits are shown in Table 2, in rows labelled Ensembles. As one would expect, the RMSE for the ensembles are larger than the long-time mean profiles. The wake law errors are smaller than the power law with a smaller standard deviation (SD). For tidal data, the RMSE shows little variation between ebb and flood or between the three ADCPs. The fit for wind data also show a better fit for the wake law. As expected, the RMSE is larger for the wind profiles with considerably larger variance.

To better compare the ensemble errors for the two models, we plot the cumulative distribution function (cdf) in Fig. 3. Remarkably, when the wake law is fit to the ADCP data, over 75% of the ensembles have an RMSE of less than 1%. For the power law, only 35% of the ADCP ensembles have an RMSE < 1%. For the wind data, the errors are larger but still promising. For the wake law 74%

of the ensembles have an RMSE of less than 2%. For the power law, only 30% of the ensembles have an RMSE < 2%.

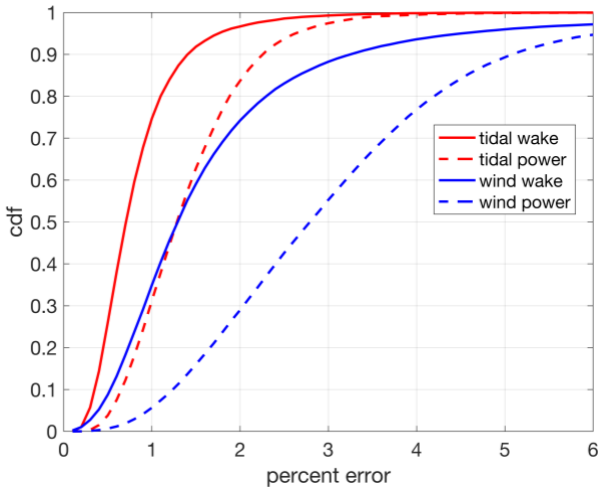

Fig. 3 Comparison of the cumulative distribution function of the ensemble fit RMSEs (%) for the wake and power law fits.

H. Parameter Values

For the parameter discussion below, we consider only values that resulted in a "good fit" as determined by the RMSE. For the tidal flow, the wake law RMSE was required to be less than 1.35% and the power law RMSE less than 2.15%. In both cases, 87% of the ensembles met this requirement. For the wind data, the RMSE cut off values were 2.1% and 4% for the wake and power laws, respectively, with 75% of the ensembles meeting the requirement.

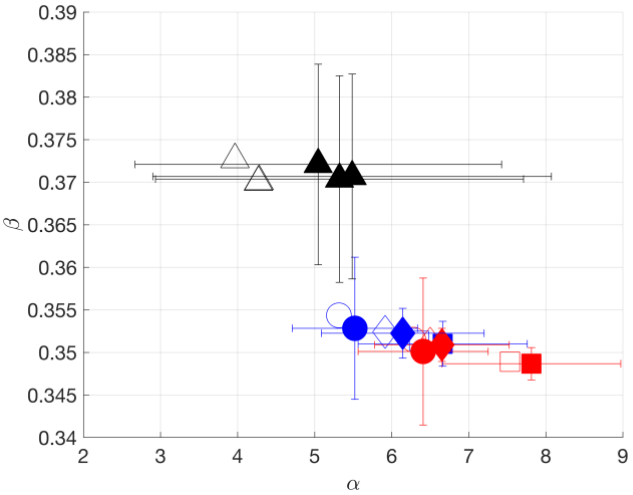

Fig. 4 Values of α and β for power law curve fitting. Red is tidal flood data; blue is ebb; and black is wind. The symbols represent the three different ADCPs sites and the one wind site for three different years. Solid symbols are the mean of ensemble fits with one SD error bars; open symbols are for the fit to the long0term average profiles.

In Fig. 4, we plot the two parameters of the power law fit, α and β, for all ensembles that had a low RMSE, as defined above. For the tidal data, we see that the mean value of α varies from 5.5 to over 7.8; combining all ensembles yields a mean value of 6.58±1.20. The values of α is higher on flood for all 3 ADCPs, but the difference between ebb and flood is within one standard deviation. As the ensemble fits gives values of α slightly larger than the value found from the mean profiles. The values for α are similar to the previous results. Sentchev et al. [2] found values ranging from 6.4 to 8. Lewis et al. [1] found mean values of 7.1±1.2 and 7.1±2.2. Naberezhnykh et al. [16] found α values of 5 or 6 the ebb and flood profiles for two ADCPs also located in the FORCE CLA in similar water depths.

The wind results are remarkably consistent over the 3 years. The mean values of α from the ensembles are larger than the value calculated from the mean profile, an indication that mean profile includes some outliers, profiles that the models do not fit well. As expected for the more variable wind, the error bars are larger. And, in comparison to the tidal value, the value of α is lower, the yearly means varying between 5 and 5.5.

In terms of the parameter, β, we see in Fig. 4 that the value varies over a very small range for both the tidal and wind data. This is to be expected for normalized flow – if the depth averaged mean of the flow is fixed, then the value of β is restricted to a small range.

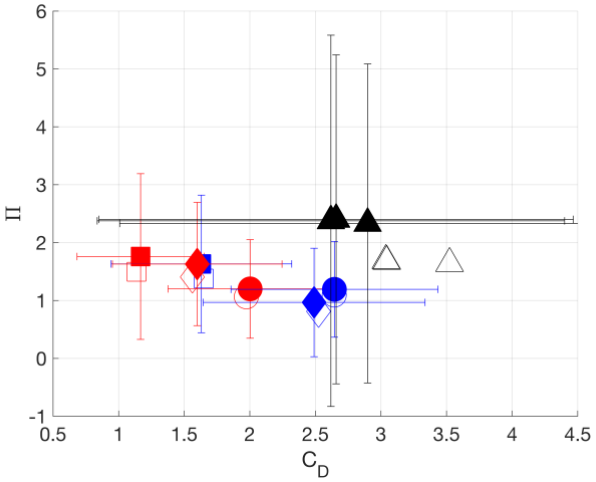

Fig. 5 Values of Π and $C_D(10^{-3})$ for wake law curve fitting. The error bars represent one standard deviation. Colours and symbols as in Fig. 4.

In Fig. 5 we plot the values of the wake law parameters Π and C_D. For the tidal flow, the mean values of Π in Fig. 5 vary from 0.97 to 1.76, with an overall mean value of 1.42 ± 1.13. The value are considerably higher than the canonical value of 0.55 used in [3] and found in Coles' original work [4]. For the wind data, once again the values across the three years are very consistent with means from 2.33 to 2.40, notably higher than the tidal values. The values for the wind profiles have a large SD, 2.75 to 3.21, again reflecting the much larger variation in the profiles.

A positive value Π indicates that the flow is faster than a logarithmic profile. The values of Π are positive for 95% of all tidal ensembles and 85% of wind profiles. The wake law does allow for profiles with reverse shear, $\frac{du}{d\eta} < 0$, if $\Pi < -9/8$. Of the profiles with a low PMSE, only 2 of the tidal profiles and 2.6% of the wind profiles satisfied this

condition. This is not to say that there are no ensembles with reverse shear. The form of the wake law used here restricts the potential of modelling reverse shear – so the RMSE will be large if the profile has large reverse shear. It should be noted that the wake law model given in (2) can be adapted to enforce different boundary conditions at $\eta = 1$, shifting the value of shear that can be modelled.

For the bottom drag, C_D, the mean values for the tidal flow range from 1.17 to 2.64 (all values for the drag are multiplied by 10^{-3}), with the overall mean 1.87 ± 0.86. The values on ebb are larger than the values on flood, but with the difference exceeding the SD only for one ADCP. The range of observed C_D values contain the typical drag coefficient value ($C_D = 2.5$) used in numerical models of the site, but the large variation requires further investigation. For the wind data, the drag values are slightly higher than the tidal values, once again with a high SD. For all ensembles we have a value of 2.7±1.8. The large amount of variation is likely the result of both the lack of measurement data near the bottom boundary and the variability in flow conditions due to thermal effects.

IV. Discussion

The results above illustrate a few key points about the vertical profiles of the flow at the Minas Passage site and the wind data at the Cabauw. For the tidal data, the normalization is a critical part of the analysis, in essence it removes the tidal signal from the results. allowing the vertical profiles at different times to be directly compared and averaged. The impact of normalization on the wind data is similar, but it does not remove the effects of temperature variations that play an important role in the stability of the atmospheric boundary layer.

The fact that both the power law and the wake law capture the profiles with such small RMSE for most of the ensembles is strong evidence that the flow in Minas Passage is a boundary layer flow, with little influence from surface forcing. Somewhat surprising, the same is true for the wind data, though with larger RMSEs.

The wake law does capture vertical profiles with a lower RMSE than the power law. The wake law also does a better job of representing the near bottom flow, calculates the friction velocity and allows for the calculation of the bottom drag. However, this comes at the cost of fitting an additional parameter.

The fitted parameter values for the tidal flow found here have similar properties to other studies. And with the wind normalized in the same manner, we also get similar parameter values. It is worth remarking that the lower values of α and higher values of Π indicate a stronger shear in the wind data and, as a result, further deviation from the logarithmic profile. For both the tidal and wind data the parameter variations over the individual ensembles are larger than the variations between the different data sets examined. One can infer that the vertical profiles are sensitive to short time variations, which is reasonable given the high level of turbulence.

For the tidal data, averaging the ensembles first and then fitting the models gave almost identical parameter values to fitting the models first and then averaging the parameters values. This gives confidence in the robustness of the modelling process. For the wind data, there was a larger difference in the two approaches, indicating that there are high speed profiles that are quite different than the models.

In conclusion, both the power law and wake law models are useful tools for examining the vertical profiles of tidal and wind data. This initial research suggests that further analysis of both wind and tidal across different sites is warranted.

References

[1] M. Lewis, S. P. Neill, P. Robins, M. R. Hashemi, and S. Ward, "Characteristics of the velocity profile at tidal-stream energy sites," *Renew. Energy*, vol. 114, pp. 258–272, Dec. 2017, doi: 10.1016/j.renene.2017.03.096.

[2] A. Sentchev, T. D. Nguyen, L. Furgerot, and P. Bailly du Bois, "Underway velocity measurements in the Alderney Race: towards a three-dimensional representation of tidal motions," *Philos. Trans. R. Soc. A*, vol. 378, no. 2178, p. 20190491, 2020.

[3] I. A. Milne, J. M. R. Graham, and D. S. Coles, "On the scaling of turbulence in a high Reynolds number tidal flow," *J. Fluid Mech.*, vol. 915, p. A104, May 2021, doi: 10.1017/jfm.2021.169.

[4] D. S. Coles, "The law of the wake in the turbulent boundary layer," *J. Fluid Mech.*, vol. 1, no. 2, pp. 191–226, doi: 10.1017/S0022112056000135.

[5] Lilli Enders, and Richard Karsten, "Improved Modelling for Vertical Profiles of Flow Speed in a Turbulent Tidal Channel," in *Proceedings of the 15th European Wave and Tidal Energy Conference*, Bilbao, Spain, 2023.

[6] L. Enders, "Flow Characterization at a Turbulent Tidal Energy Site in Minas Passage, Bay of Fundy," MSc Thesis, Acadia University, 2022.

[7] "KNMI Research - Observations & Data Technology - CESAR (Cabauw) and wind." https://www.knmi.nl/research/observations-data-technology/projects/cesar-cabauw-and-wind (accessed Jul. 20, 2023).

[8] G. I. Barenblatt, A. J. Chorin, and V. M. Prostokishin, "Turbulent flows at very large Reynolds numbers: new lessons learned," *Phys.-Uspekhi*, vol. 57, no. 3, p. 250, Mar. 2014, doi: 10.3367/UFNe.0184.201403d.0265.

[9] J. M. McMillan, A. E. Hay, R. G. Lueck, and F. Wolk, "Rates of Dissipation of Turbulent Kinetic Energy in a High Reynolds Number Tidal Channel," *J. Atmospheric Ocean. Technol.*, vol. 33, no. 4, pp. 817–837, Apr. 2016, doi: 10.1175/JTECH-D-15-0167.1.

[10] R. G. Lueck and Y. Lu, "The logarithmic layer in a tidal channel," *Cont. Shelf Res.*, vol. 17, no. 14, pp. 1785–1801, Dec. 1997, doi: 10.1016/S0278-4343(97)00049-6.

[11] T. Von Kármán, *Mechanical similitude and turbulence*. National Advisory Committee for Aeronautics, 1931.

[12] M. P. Schultz and K. A. Flack, "The rough-wall turbulent boundary layer from the hydraulically smooth to the fully rough regime," *J. Fluid Mech.*, vol. 580, pp. 381–405, Jun. 2007, doi: 10.1017/S0022112007005502.

[13] J. Guo, "The Log-Law of the Wall in the Overlap from a Functional Equation," *J. Eng. Mech.*, vol. 149, no. 2, p. 06022005, 2023.

[14] S. Emeis, *Wind Energy Meteorology: Atmospheric Physics for Wind Power Generation*. Springer, 2018.

[15] L. Liu, S. N. Gadde, and R. J. A. M. Stevens, "Universal Wind Profile for Conventionally Neutral Atmospheric Boundary Layers," *Phys. Rev. Lett.*, vol. 126, no. 10, p. 104502, Mar. 2021, doi: 10.1103/PhysRevLett.126.104502.

[16] A. Naberezhnykh, D. Ingram, I. Ashton, and J. Culina, "How Applicable Are Turbulence Assumptions Used in the Tidal Energy Industry?," *Energies*, vol. 16, no. 4, Art. no. 4, Jan. 2023, doi: 10.3390/en16041881.